

Intermodulation Distortion Analysis for DFB Lasers

T.Okuda, H.Yamada, T.Torikai and T.Uji

KANSAI Electronics Research Laboratory, NEC Corporation
2-9-1, Seiran, Otsu 520, Japan

The modulation distortion mechanism in DFB lasers due to longitudinal electrical field nonuniformity along the laser cavity was theoretically clarified. The theoretical yields for ensuring low distortion characteristics were calculated for various device structures. The coupling coefficients (κL) and facet reflectivities were specified for designing low distortion DFB lasers.

1 INTRODUCTION

Subcarrier multiplexing has become a very attractive technique for fiber optic loop applications, such as CATV and microcellular mobile communication systems^{1,2}). In such systems, low intermodulation distortion characteristic DFB lasers are required to ensure high carrier to noise ratio. The distortions are strongly related to relaxation oscillation and the longitudinal electrical field nonuniformity in DFB laser. So far, the former mechanism has been intensively studied³). However, the latter has not yet been investigated in detail.

The purpose of this work is to theoretically clarify the distortion mechanism and to provide an optimum high yield low distortion DFB lasers design for practical use. The light output-current (P-I) nonlinearity due to field nonuniformity along the laser cavity was investigated. Consequently, low distortion characteristics were derived under certain coupling coefficient (κL) and facet reflectivities conditions.

2 MODEL AND CALCULATION

An analyzed DFB laser model is shown in Fig.1. In order to consider longitudinal electrical field distribution along the laser cavity (See Fig.1), the coupled-equations were solved by the F matrix method⁴).

The grating phase uncertainties at both facets were also taken into account in this calculation, since grating phases on cleaved facets which affect

phase conditions for laser oscillation and electrical field distributions are uncontrollable in DFB lasers.

As an example, calculated P-I characteristics and longitudinal electrical field distributions are shown in Fig.2 and Fig.3, respectively. In both figures, (a) and (b) are the calculated results for a device with the same structure except for facet phases.

In case (a), the P-I curve shows good linearity, and the electrical field is almost uniform along the cavity. Moreover, the field is fairly fixed versus current injection. On the other hand, in case (b), the P-I curve shows nonlinearity, and the electrical field is nonuniform. That is, a large change in field distribution versus current injection obviously causes the nonlinearity in the P-I curve.

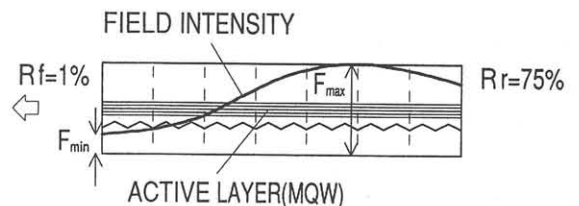


Fig.1 DFB laser model. The DFB laser consists of a homogeneous grating along the cavity and AR and HR coated facets. The field uniformity in the laser cavity was defined as a maximum and minimum intensity (F_{min}/F_{max}) ratio.

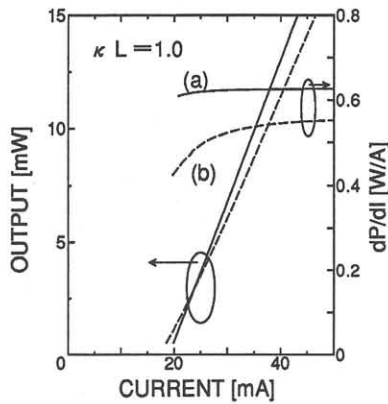


Fig.2 Calculated P-I and dP/dI characteristics for devices with different facet phases, (a) $\phi_f = -\frac{5}{8}\pi, \phi_r = -\frac{1}{4}\pi$ and (b) $\phi_f = -\frac{3}{4}\pi, \phi_r = \frac{3}{8}\pi$, respectively.

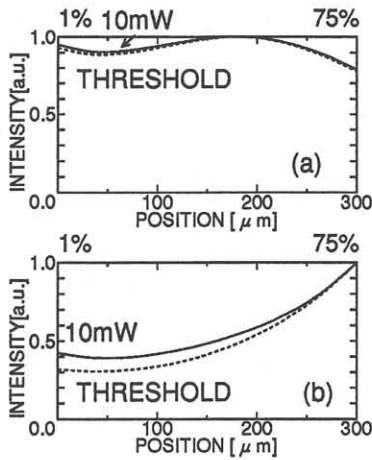


Fig.3 Longitudinal electrical field distributions at threshold (dashed line) and 10mW output power (solid line). The facet phases for (a) and (b) are the same as in Fig.2.

3 ANALYSIS

3.1 Intermodulation distortion

Intermodulation distortions are derived from the P-I curve calculated above. The P-I curve is expanded into the Taylor series around a bias point (I_b),

$$P = P_0 + A_1(I - I_b) + \frac{A_2}{2}(I - I_b)^2 + \frac{A_3}{6}(I - I_b)^3 + \dots \quad (1)$$

, where I is the current, P is the light output power, P_0 is the averaged light output power, and A_1, A_2 and A_3 are expansion coefficients. The optical modulation index (OMI) is defined as,

$$OMI = \frac{A_1 I_m}{P_0} \quad (2)$$

, where I_m is modulation current. For subcarrier multiplexing, the modulation index is modified into the effective OMI (OMI_{eff}). The composite second order (CSO) distortion is determined by the second order expansion coefficients,

$$CSO = N_c \frac{A_2^2 P_0^2 OMI_{eff}^2}{8 A_1^4} = N_c \frac{N A_2^2 P_0^2 OMI^2}{16 A_1^4} \quad (3)$$

, where N is the number of carriers (channels) and N_c is the number of second-order intermodulation products in a channel. The CSO distortions were calculated under 5mW light output power and 5% per channel OMI conditions, based on 42ch CATV system specifications. Figure 4 shows calculated CSO distortions for devices with the same structure involving 256 different types of facet phases as a function of field uniformity, defined by the intensity ratio (F_{min}/F_{max}), as shown in Fig.1. As seen in Fig.4, lower CSO distortion can be realized with increasing field uniformity.

3.2 κL dependence

According to the method mentioned above, the theoretical probabilities of ensuring a required low distortion, terms as yield can be obtained by calculating the distortion for the devices with various facet phases. The yield κL dependence was calculated first, since the field uniformity is strongly affected by the κL value.

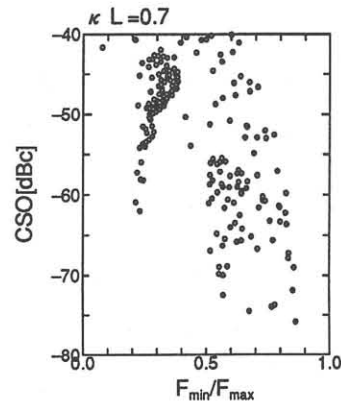


Fig.4 Calculated CSO distortions as a function of field uniformity (F_{min}/F_{max}).

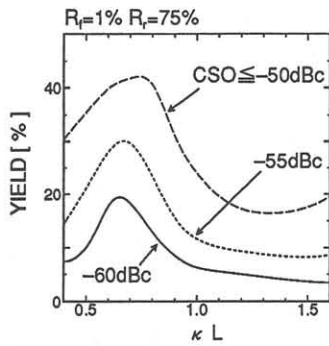


Fig. 5 Yield κL dependence. The optimum κL value exists around 0.6 ~ 0.7.

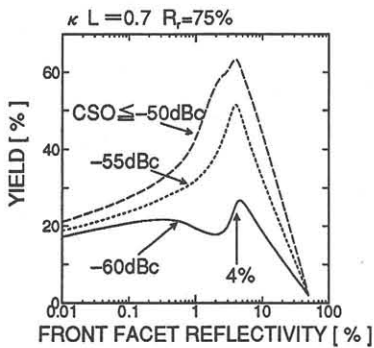


Fig. 6 Yield as a function of front facet reflectivity. The optimum front facet reflectivity is about 4%.

Figure 5 shows the yield κL dependence, calculated under three specifications: (1) $CSO \leq -50dBc$, (2) $CSO \leq -55dBc$ and (3) $CSO \leq -60dBc$. The criteria for the normalized threshold gain difference between the main mode and the next submode was employed ($\Delta\alpha L \geq 0.05$) for taking the single longitudinal mode stability into account. The optimum κL value exists around 0.6 ~ 0.7 under such conditions. Low yield is attributed to unstable single mode operation under the lower κL condition and nonuniform electrical field distribution under the larger κL regime.

3.3 Facet reflectivity dependence

Next, the yield facet reflectivity dependence was calculated. In this calculation, the κL value was fixed to 0.7, which is the optimum value mentioned above. The front and rear facet reflectivity dependencies are shown in Fig.6 and Fig.7, respectively.

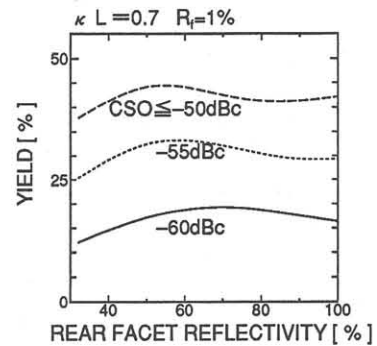


Fig. 7 Rear facet reflectivity yield dependence. There is no obvious dependence on the rear facet reflectivity.

The optimum front facet reflectivity (R_f) was about 4%, which is mainly due to single mode stability effects under the high R_f conditions. Furthermore, facet phase differences cause wide CSO distribution under the lower R_f conditions, and resulting in yield decrease.

On the other hand, the yield was almost independent from the rear facet reflectivity, as shown in Fig.7. However, R_f should be as high as possible to realize high slope efficiency, from the practical use viewpoint.

4 SUMMARY

A method for analyzing intermodulation distortion was developed. Theoretical yield for low distortion characteristics in DFB lasers was analyzed using the calculation method. The distortion mechanism due to electrical field nonuniformity along the laser cavity was clarified and then device parameters were tailored, so as to realize low distortion DFB lasers.

REFERENCES

- 1) M. Shibutani, T. Kanai, K. Emura and J. Namiki, ICC'91 (1991) 1176.
- 2) R. Olshansky, V.A. Lanzisera and P.M. Hill, J. Lightwave Technol. **7** (1989) 1329.
- 3) J. Helms, J. Lightwave Technol. **9**(1991) 1567.
- 4) M. Yamada and K. Sakuda, Appl. Opt. **26**(1987) 3474.